UAS testing in low pressure and temperature conditions

UAS testing in low pressure and temperature conditions*

Matteo Scanavino[1], Arrigo Avi[2], Andrea Vilardi[2] and Giorgio Guglieri[1]

Abstract— **The increasing demand of UAS has generated interest in the scientific community to understand how the environmental parameters affect performance of these emerging vehicles. A bias in the existing tests has been the non-reproducibility of the same climatic conditions. Therefore, UAS have not been fully exploited by the marker so far. Standard protocols for UAS testing in unconventional weather conditions have not been investigated from both industry and academic research. Temperature and pressure are environmental parameters that affect the aerodynamics of Unmanned Aircraft Systems (UAS). Low Reynolds numbers are common for small scale UAS and have a strongly influence on propeller and vehicle capabilities. In the past years, experimental studies on the effects of low Reynolds numbers have been carried out in wind tunnel facilities in conventional atmospheres (ambient temperature and pressure). Moreover, the complexity of the aerodynamic field results in propeller and full vehicle performance prediction methods with limited accuracy. In this paper an experimental setup inside a climatic and hypobaric laboratory is used to highlight temperature and pressure influence on single propeller and full vehicle performance in static conditions (hover). Test results are discussed and provided to the reader, highlighting the complexities of the measurements when extreme temperature and low pressure are set. The main contribution of this study is a set of experimental data to pave the way for a deep investigation on harsh environmental conditions on UAS propulsion system.**

Index Terms— **Propeller and UAS Performance, Harsh Environmental Conditions, Test Stand**

I. INTRODUCTION & RELATED WORK

Unmanned Aircraft Systems (UAS) are aerial platforms widely used for both commercial and recreational purposes. A wide range of applications [1] are possible including precision farming, surveillance and monitoring as well as delivery. In the next future, further developments will be possible thanks to the integration of UAS with emerging technologies (i.e. network system and Beyond Visual Line of Sight [2]) so that unmanned vehicles are at the beginning of their explosion.

The increasing demand of UAS has generated interest within the scientific community to improve vehicle capabilities. In the past years, efforts were made to enhance autopilot performance with guidance, control and navigation algorithms able to operate the vehicle with limited pilot intervention. Moreover, experimental studies focused on the characterization of off-the-shelf propellers, brushless motor and more in general the identification of the UAS platforms [3] to improve simulation models. To fully exploit the potential of UAS technology in the upcoming application scenarios further studies are required to answer current research questions. As an example, the development of an Unmanned Traffic Management (UTM) system is a challenge to enable a safe low-altitude airspace for UAS applications. In this context, experimental studies on small UAS vehicle were recently performed by NASA. In [4] the authors focus on the Failure Mode Effects Analysis (FMEA) for commercial aerial vehicles to quantify the level of risk associated with UAS vehicles and components. Moreover, for the implementation of a UTM system it is important to understand the capabilities of unmanned aerial system in a range of different environmental conditions. Power consumption, propulsion system efficiency as well as UAS behaviour in both conventional and unconventional weather are major topics for the next generation of unmanned aerial vehicles. Experimental data are needed to fill the gap of current research on UAS performance.

The authors in [5] focus on the aerodynamic characterization of propellers for small UAS applications. The effect of low Reynolds number on twenty-seven off-the-shelf propellers designed for UAS (fixed and rotary wing platforms) in both static and windy conditions are studied in terms of thrust and power coefficients. Low Reynolds numbers (below $100,000$) are common for small UAS propeller, owing to their limited chord dimensions and motor speed range. Results show that as the Reynolds is lowered, the propeller performance are degraded in terms of reduced thrust coefficient. The experimental research in [6] describes a 2D airfoil visualization technique (fluorescent oil flow visualization) to investigate the aerodynamic flow at Reynolds numbers common for UAS applications. The authors explain that the aerodynamic performance (lift, drag and efficiency) are affected by the *laminar separation bubble*. The complexity of the flow is the result of boundary layer separation and its reattachment after the transition to turbulent conditions. Wind tunnel propeller analyses [9] have provided a complete database of performance for propellers installed on small UAS. Recently, full vehicle and isolated rotor tests have been performed at NASA Ames Research Centre [10] to measure force and moments as well as electrical power consumption as a function of wind speed and UAS attitude. The objective of NASA test program was to collect a high quality set of data and investigate the capabilities of unmanned vehicles under a range of wind conditions. Other environmental

[1]M. Scanavino is with the Department of Mechanical and Aerospace Engineering, Politecnico di Torino, C.so Duca degli Abruzzi 24, 10129 Torino, Italy, Corresponding author (e-mail: matteo.scanavino@polito.it)

[2]A. Avi is with terraXcube, Eurac Research, Via Ipazia 2, 39100 Bolzano, Italy

[2]A. Vilardi is with terraXcube, Eurac Research, Via Ipazia 2, 39100 Bolzano, Italy

[1]G. Guglieri is with the Department of Mechanical and Aerospace Engineering, Politecnico di Torino, C.so Duca degli Abruzzi 24, 10129 Torino, Italy

parameters (such as temperature and pressure) have never been investigated with respect to UAS performance. For this reason, many of the existing applications designed for UAS have not been fully exploited by the market so far. Moreover, a bias in the existing tests has been the non-reproducibility of the same climatic conditions. To fill the gap, the aim of *DronEx* project [14] by Eurac Research is to focus on how harsh environments (i.e. low temperature and low pressure) influence unmanned vehicle performance. This paper is an extension of the preliminary study in [15]. In the previous work, we focus on propeller performance at low temperature and pressure, highlighting thrust and electrical power curves with respect to motor speed and environmental conditions. In this paper the isolated rotor and full vehicle (quad-rotor) performance are both investigated for different combinations of temperature and pressure. In total, 26 different atmospheric conditions are simulated in *terraXcube*, a dedicated climate-controlled laboratory in Bolzano, Italy. The primary objective of this study is to leverage this environmental simulator in order to fill the gap in current experimental research and provide a systematic approach on UAS performance analysis in unconventional weather conditions. The ultimate goal is to collect a set of data to improve vehicle design and provide insight on UAS behaviour under unconventional weather conditions. This paper is structured as follows. Section II presents the experimental setup, including the test facility and sensors. Test results are reported and discussed in Section III, conclusions and future works are summarized in Section IV.

II. METHODS & PROCEDURES

This paper focuses on the experimental evaluation of temperature and pressure effects on propeller and full vehicle performance in static conditions. All the measurements take place inside *terraXcube* [16], a hypobaric climatic laboratory where it is possible to set extreme environmental conditions. The facility was built in 2018 for medical purposes; however, industrial tests are possible thanks to the capabilities of this simulator. It is important to highlight that *terraXcube* is not designed for wind tunnel measurements. For this reason, all the tests are taken in static conditions (hover). The dimensions of the test section (LxWxH, 12m x 6m x 5m) are exploited to install two test stands (Figure 1) inside the chamber for the propeller and full vehicle. In this way, testing time is reduced. The facility allows to control many environmental parameters (such as humidity, solar radiation, rain and snow) but for the purpose of this study, temperature (from -40°C to 40°C) and pressure (from 1013 mbar up to 300 mbar) are the quantities we focus on.

The propeller and motor used for the tests are representative of small/medium scale UAS. The T-Motor $15'$ x $5'$ is a carbon fiber propeller used by professional drone applications. Even tough nylon propellers are more common for hobbyists and researchers due to their low cost, the T-Motor is chosen as it is possible to compare the data with the experimental test performed by Russell [10]; furthermore, they report the propeller geometry (chord, twist and airfoil distribution) that will be used for numerical analysis. The

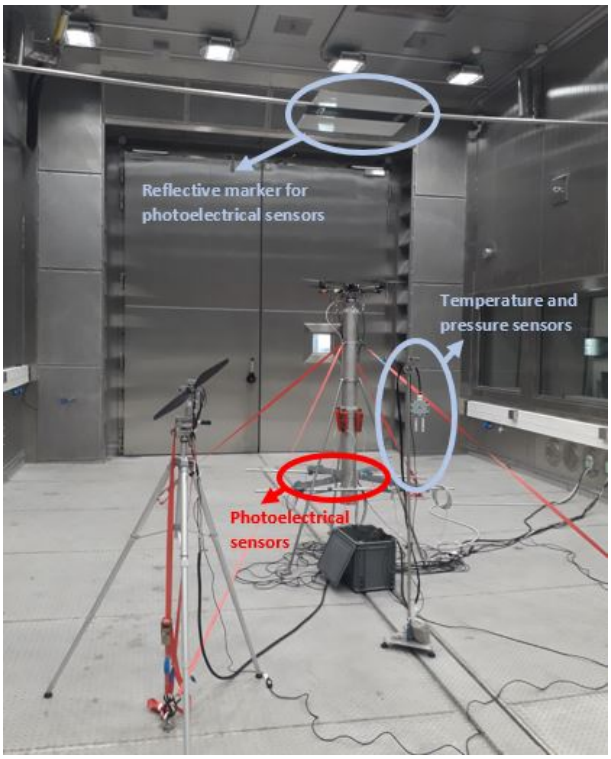

Fig. 1: Test stands for propeller and full vehicle measurements inside *terraXcube*.

electric brushless motor is the T-Motor MN3508 380KV [19] with a maximum power of 310W. This is the same motor installed in the quad-rotor used for the full vehicle tests. This vehicle is a professional UAS with a Maximum Take-Off Weight (MTOW) of 1.7 kg and is employed in crop field monitoring with optical sensors. The Electronic Speed Controller (ESC) used for the propeller test is a Turnigy Push 30A, while the full vehicle uses the Flyduino KISS ESC.

A. Instrumented Test Stand for Propeller

To evaluate the performance of the isolated rotor, the RCBenchmark 1585 [17] dynamometer is used. This simple test stand allows to measure thrust, torque, motor speed (electrical estimate based on phase current sensing) and electrical power. The motor torque is measured by two load cells, given the distance between them [20]. The RCBenchmark dynamometer is designed to measure propeller performance in standard environmental conditions. For this reason, the propeller tests are limited above 0°C, as temperature affects the load cells response. The propeller and motor are mounted to avoid airflow interaction with the support rod, as depicted in Figure 2. In this configuration, the load cell is compressed by the propeller thrust; the motor and electronic speed controller are not immersed in the propeller downstream flow. This is not the conventional motor installation for UAS propulsion systems, however this configuration is preferred to reduce the aerodynamic effects, as suggested by [21]. The PWM signal to the electronic speed controller is automatically set by a computer in the control room and consist of a

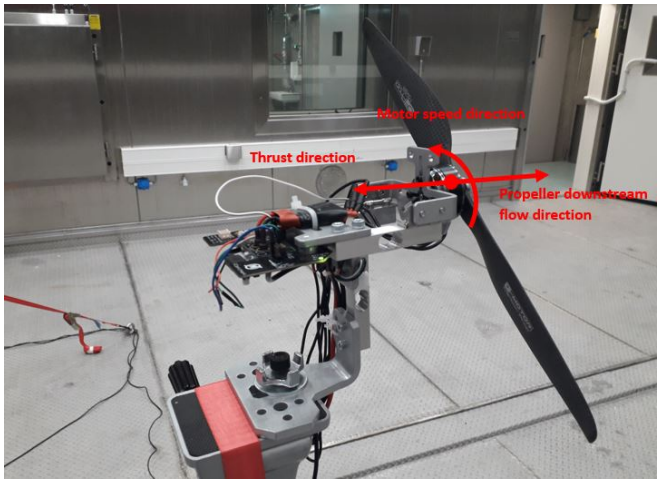

Fig. 2: Propeller mounting on the RCBenchmark thrust stand.

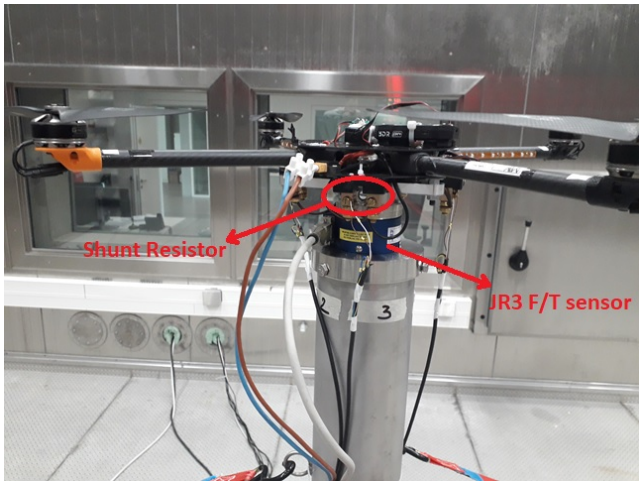

Fig. 3: Experimental setup for quad-rotor performance measurements.

step sequence from 1400us up to 2000us equally subdivided in the 10 parts. Each step is made by a settling time of 3s after which a new log entry is recorded. To reduce noise, 20 samples are averaged and recorded. To avoid battery charging time, the electrical power is provided by a DC power supply placed in the control room outside the test section.

B. Quad-rotor Instrumented Test Stand

Isolated rotor tests provide insight on propeller low Reynolds aerodynamics; however, full vehicle measurements are important as they account for the interaction between rotor wakes and vehicle airframe as suggested by [10], [11] and [12]. To investigate the performance of a full vehicle, a custom fabricated test stand is used (Figure 3). It consists of a welded-steel construction with a central hollow tube filled with sand. The test stand is anchored to the floor with straps to reduce mechanical vibrations. The overall structure is similar to the test bench described by Conyers et al. in [22] and [23] for ground and ceiling effect evaluation. The 30E15A4 JR3 [25] Force/Torque sensor (F/T) is attached to the top of the test stand; a custom designed interface plate is rigidly mounted between the load cell and copter frame. The sensor is able to measure thrust and torque generated by UAS along three directions. The sensor capacities are ± 200 N (F_x and F_y), ± 400 N (F_z) and ± 16 Nm (T_x, T_y and T_z) with resolutions of 0.025 N, 0.05 N and 0.002 Nm respectively. The minimum operating temperature of the load cell is -40°C, which is also the minimum temperature reached during the tests. The raw data from the sensor are sampled every 100 ms, decoupled and digitalized by the F/T electronics placed in the control room. All the F/T signals are processed through a low pass filter with a cutoff frequency at 0.5Hz to remove noise due to mechanical vibrations. Motor speeds are measured using four photoelectric sensors (Sick WLAP16 [26]) which sense the blade passing frequency. A reflective square-marker is placed near the ceiling (Figure 1). In this way, non-intrusive measurements of the motor speed are possible without any additional probes on the propellers. The photoelectric sensors provide an impulse each time the light beam is interrupted by the blade. The blade passing frequency is converted in to motor speed by a dedicated counter module of the data acquisition system (DAQ). Initial attempts to measure motor speeds with optical tachometers resulted in unstable measurements due to light and environmental conditions so that photoelectric sensors were preferred. Shunt resistors are used to sense the electric current flowing in each motor. Moreover, the total current and voltage are measured by an additional shunt resistor and voltmeter placed between the power supply and the vehicle power unit. As the objective of the test is the measurement of overall performance, the on-board autopilot is bypassed and the motor PWM cables are directly connected to the RC transmitter to the throttle channel. The test engineer controls the UAS throttle at predefined values; the same throttle levels are set for all the environmental conditions. All the other measurements are recorded through an Ipetronik DAQ at 10 Hz, with the only exception of the F/T sensor which is directly connected to a computer through its electronic interface. To avoid battery charging time, a DC power supply is used and placed in the control, outside the test section. The supply voltage is controlled and set to 16.8V, with a maximum output current of 70A. As a result, this solution allows to reduce transient voltage fluctuations which are common when using Li-Po batteries.

C. Testing Procedures

During the tests, different combinations of temperature and pressure are simulated in the test section to study the influence of Reynolds number on performance. The temperature considered are $+40$ °C, $+20$ °C, 0 °C, -20 °C and -40 °C; for all these temperatures, the equivalent altitudes set are 0 m (sea level), 1500 m, 3000 m, 4500 m and 6000 m. Moreover, the minimum pressure of 300 mbar (9000 m) at 20 °C is considered to highlight extreme low pressure effect. Figure 4 shows the air densities corresponding to the environmental conditions simulated. The high densities correspond to low temperature and high pressure conditions; the opposite for

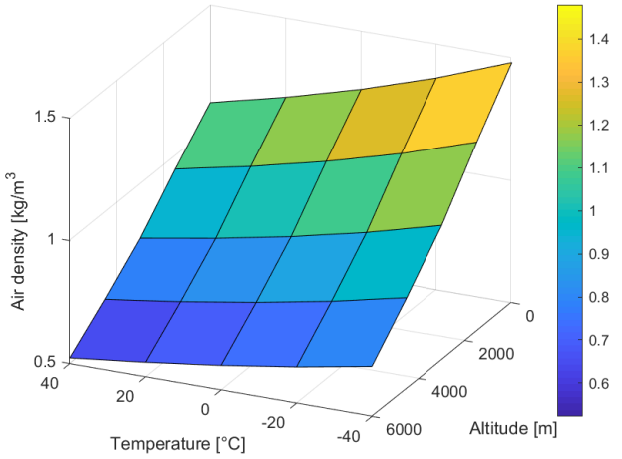

Fig. 4: Air densities set in test chamber for the tests.

high temperature and altitude. In total, 26 different climatic conditions are investigated for the full vehicle. For the isolated rotor, test matrix is limited to $+40$ °C, $+20$ °C and 0 °C: measurements below 0°C are affected by the unstable response of the dynamometer.

When setting a new temperature, all the measurements are taken after 15 min from reaching the set-point condition. This time is required for the stabilization of the load cells. terraX-cube allows to set a temperature rate of change of 30 °C$/h$, while for pressure the equivalent rate of climb/descent is 5 m/s. To reduce testing time, we set a temperature and investigate all the altitudes at that temperature. In this way, we are able to enter inside the test section before low pressure are simulated and make the necessary adjustments if unexpected behaviours are experienced. The environmental matrix is simulated from high to low temperatures, from sea level to the maximum altitude. When stable conditions are obtained, the single rotor and full vehicle tests are executed independently. Firstly, the single rotor is powered and the automatic PWM generator script is launched. The same PWM signals are sent to the electronic speed controller for a comparison at different environmental conditions. Secondly, the full vehicle is tested. This is done using a Remote Controller commanded by the test engineer in the control room. Four throttle levels (50%, 66%, 80% and 100%) are set for all the tests. Each throttle is sampled for 30 s for stable flow conditions. Before starting a new recording, all the sensors are checked to be sure everything is working properly.

Technical problems related to the environmental conditions arose during the test, especially when low pressures were set. A common issue revealed at high altitude was the behaviour of the electronic speed controllers: it was common that one of the motor was spinning visibly slower than the others. The ESC calibration was performed each time the motor speeds logged by the DAQ system were not synchronized. Another problem was the de-soldering of the motor phases by the ESC connectors, probably due to *cold welding* and mechanical stress resulting from low temperatures and pressures.

III. RESULTS

This section presents performance data for the isolated rotor and full vehicle. Thrust and mechanical power are given as a function of motor speed for all the altitudes (at constant temperature) and temperatures (at constant altitude) to investigate their individual influence on isolated propeller and complete UAS. For all the atmospheres, propeller performance are discussed in term of thrust and torque coefficients (Equation 1) with respect to the Reynolds number,

$$c_T = \frac{T}{1/2\rho D^4 n^2}, \qquad c_Q = \frac{Q}{1/2\rho D^5 n^2}, \tag{1}$$

where T is the thrust, Q is the propeller torque, ρ is the air density, n is the motor angular speed in [rev/min] and D is the propeller diameter. c_T and c_Q are dimensionless quantities related to the propeller geometrical design, advance ratio and Reynolds number. The latter is computed at 75% of the propeller radius according to the Equation 2

$$R_e = \frac{\rho v c}{\mu} \tag{2}$$

where v is the velocity at 75% of the propeller radius given by the motor angular speed, c is the propeller chord (at 75% of the propeller radius) and μ is the air viscosity computed using Shuterland's Law. For the full vehicle case, the thrust coefficient is computed based on the the average angular rate of the four rotors. Moreover, as the total torque acting on the UAS is close to zero, the electrical power coefficient is given with respect to the Reynolds as defined in Eq.3,

$$c_P = \frac{P_e}{1/2\rho D^5 n^3} \tag{3}$$

where P_e is the total electrical power required by the vehicle. The c_P accounts motor efficiency and mechanical power coefficient.

A. Isolated Propeller

Pressure and temperature effects on the mechanical performance of the isolated rotor are presented separately. Pressure effects are considered at a constant temperature; then, temperature influence is evaluated at constant pressure. Finally, the combined atmospheres (all the temperature and pressure set during the tests) are presented in term of thrust and torque coefficient with respect to the Reynolds number.

1) Pressure test: Figure 5 shows the thrust-speed curve for the isolated rotor test at different altitudes, 20 °C constant temperature. As the altitude is increased, the thrust generated by the propeller is reduced as direct consequence of the air density decreasing. At constant temperature, the air density is directly proportional to air pressure. At 9000 m, the thrust generated by the propeller is up to 55% of the maximum thrust available at sea level. At the same time, the motor

speed increases despite the same PWM command signals are sent to the electronic speed controller. The higher the altitude, the faster the motor spins as a direct consequence of the smaller torque load acting on the propeller. Given a desired thrust level, the higher the altitude the more power required by the motor, as clearly visible by the square markers in Figure 6, due to faster motor speed needed to reach the same thrust. As an example, a 40% increase in the mechanical power is required to generate 7 N at 4500 m with respect to sea level conditions.

2) Temperature tests: Temperature effect on propeller thrust and mechanical power are shown in Figure 7 and 8. At constant pressure (990 mbar), the air density is inversely proportional to the temperature. The lower the temperature, the higher the air density resulting in more thrust. Given the same thrust level, high temperature result in more mechanical power required by the propeller as the air density decreasing is compensated by faster motor speed. The higher the temperature, the more power is required to generate the same thrust.

3) Reynolds effect on thrust and torque coefficients: To summarize all the environmental conditions, thrust and torque coefficients are given as a function of Reynolds number in Figure 9 and 10 respectively. For the environmental test matrix set and motor speed, the Reynolds is in the range $40,000 - 150,000$. Low Reynolds numbers represent slow motor speeds and small air densities (high temperatures and low pressures). The thrust coefficient in Figure 9 shows a linear behaviour. The c_T trend is similar to the static thrust coefficient measured by [5] for small UAS propellers. At low Reynolds number, the viscous forces have a large effect on the airfoil capability to generate lift. The study performed by [24] on the effect of Reynolds number on airfoils shows that low Reynolds usually result in smaller lift and increased drag coefficients. This is confirmed by the experimental data collected at low Reynolds in Figure 9. The propeller thrust is a combination of the airfoils lift and drag coefficients: low Reynolds are responsible for worst aerodynamic efficiencies owing to the larger effects of viscous forces. For this reason, smaller thrust coefficients are measured. The thrust coefficient experiences a 16% increase in the Reynolds range. On the other side, a constant torque coefficient is in Figure 10. As a result, the mechanical power coefficient does not depend on Reynolds number, in accordance with propeller data by [5] for static test conditions (hover). In conclusion, considering a constant motor speed, the thrust is directly proportional to the product of air density and thrust coefficient while the mechanical power depends only on the air density as the power coefficient is not affect by the Reynolds. A limited data dispersion is visible in Figure 9 and 10. This behaviour is strongly related to temperature effects on the RCBenchmark test stand as shown in Figure 11, where the data dispersion is more evident for temperature below at 0°C. For this reason, measurements at -20°C and -40°C are excluded; propeller tests at low temperature will be investigated with the JR3 F/T sensor in the next test campaign.

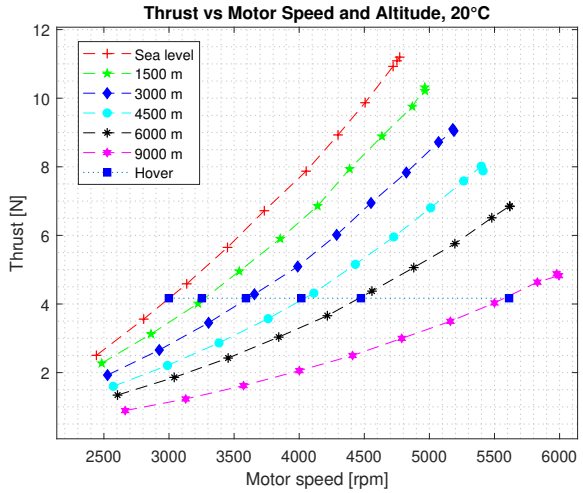

Fig. 5: Isolated rotor, Thrust - Motor Speed curve as a function of the altitude.

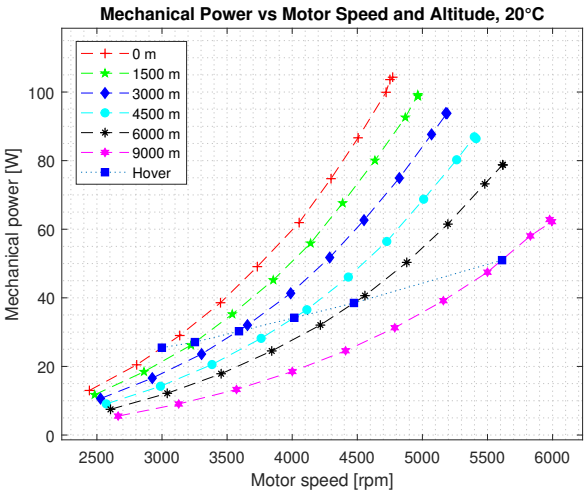

Fig. 6: Isolated rotor, Mechanical Power - Motor Speed curve as a function of the altitude.

B. Quad-rotor Performance

1) Pressure Test: As for the isolated rotor, Figure 12 shows the full vehicle thrust - average motor speed for all the altitudes at constant temperature (20°C). The dotted blue line is the thrust level required for hovering. Thrust reduction due to air density decrease is evident. Considering the maximum altitude (9000 m), the UAS is not able to take-off as the thrust generated by the propulsion system is slightly higher than the MTOW. Furthermore, as the altitude increases higher motor speeds are required to reach the hover thrust. For this reason, the electrical power (Figure13) increases and the UAS endurance is reduced.

2) Temperature Test: The UAS thrust and power performance as a function of motor speed and temperature are in Figure 14 and 15 respectively: at constant pressure, lower temperatures give higher thrust generated by the vehicle as a consequence of the air density increasing. Accordingly, the

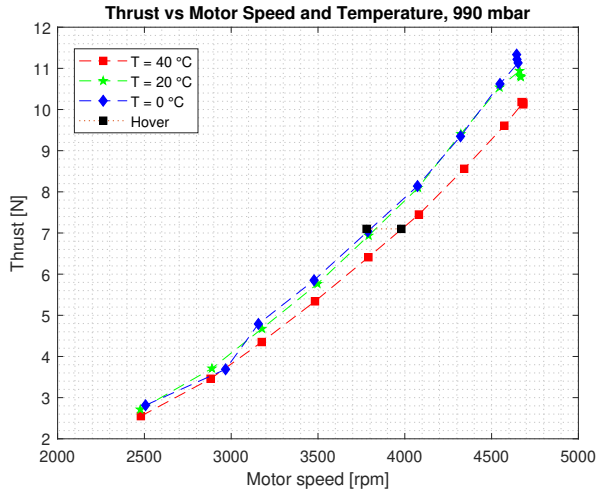

Fig. 7: Isolated rotor, Thrust - Motor Speed curve as a function of the temperature.

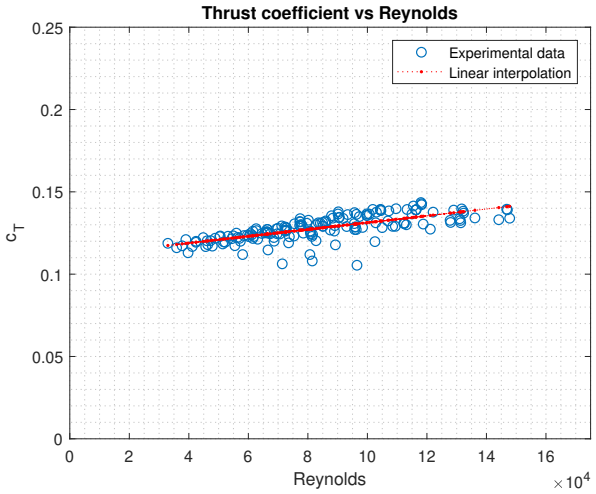

Fig. 9: Propeller thrust coefficient and Reynolds number for all the temperature and pressure.

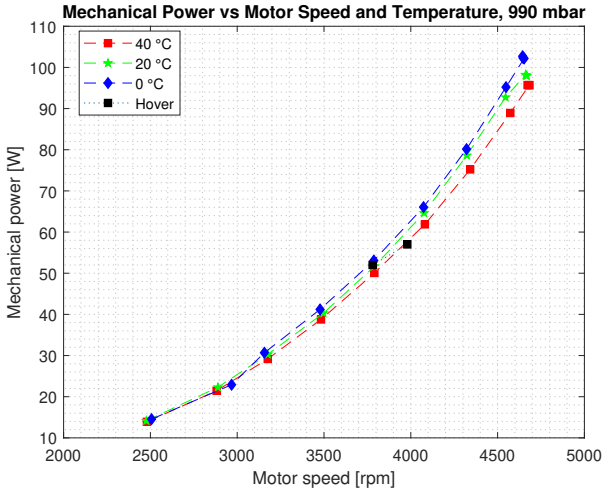

Fig. 8: Isolated rotor, Mechanical Power - Motor Speed curve as a function of the temperature.

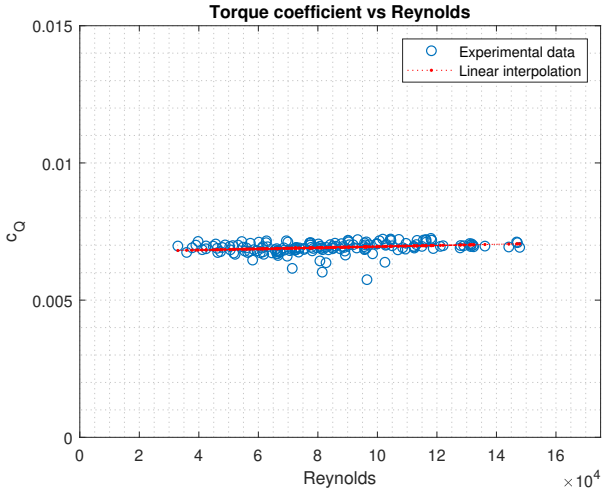

Fig. 10: Propeller torque coefficient and Reynolds number for all the temperature and pressure.

motor speed required to hover is reduced as colder temperature are set. Moreover, the electrical power required to hover the copter is smaller. However, the lower the temperature, the less efficient are the Li-Po batteries, resulting in worst vehicle performance. This effect is not highlighted in our study as a DC power supplier is used instead of batteries.

3) Reynolds effect on thrust coefficient: The UAS thrust coefficient as a function of Reynolds number is in Figure 16 for the all the environmental conditions. The blue circles are the experimental data while the red line is a linear interpolation. As for the isolated rotor, the smaller the Reynolds, the lower the thrust coefficient. The Reynolds is in the range $40,000 - 180,000$; the thrust coefficient experience a 16% increase as the Reynolds increase, the same increment computed for the isolated rotor. Moreover, the full vehicle c_T is close to four times the thrust coefficient of the isolated rotor. For the full vehicle, the electrical power coefficient is given in Figure as a function of Reynolds number. The full vehicle c_P trend is almost constant, even though a limited increase can be found as higher Reynolds are set. The electrical power coefficient accounts for the mechanical power coefficient and the motor efficiency. As a result, the propulsion system efficiency slightly affects the electrical power coefficient. During the next test campaign, the isolated rotor motor efficiency will be measured as a function of the environmental temperature and pressure. In this way, it will be possible to extract the full vehicle mechanical power coefficient from the electrical data and check that the mechanical power coefficient is not affected by the Reynolds, as suggested by the torque coefficient of the isolated rotor.

IV. CONCLUSIONS & FUTURE WORK

Temperature and pressure effects on isolated rotor and quad-rotor performance have been investigated in a dedicated test facility. A setup is built to measure thrust, torque, motor

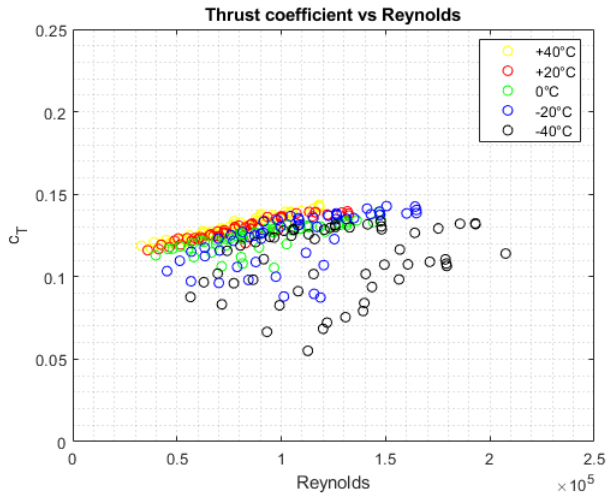

Fig. 11: Effect of low temperatures on the RCBenchmark test stand.

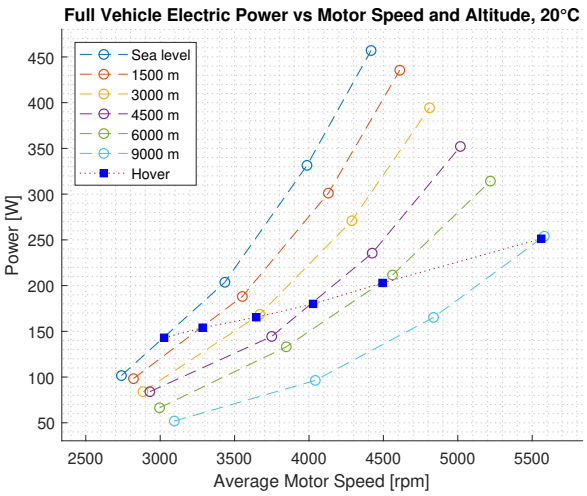

Fig. 13: Full vehicle electrical power as a function of motor speed for all the altitudes - 20°C.

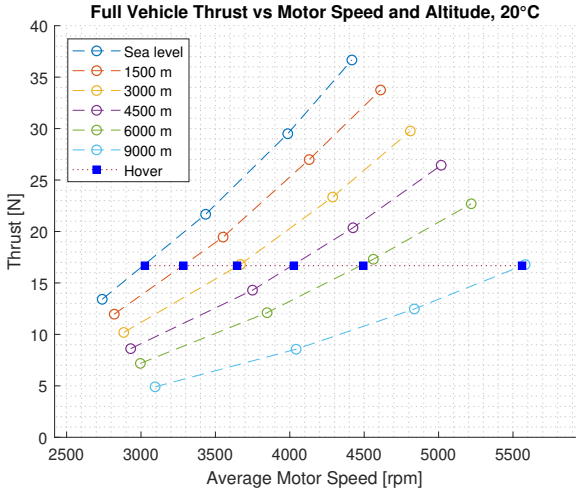

Fig. 12: Full vehicle thrust as a function of motor speed for all the altitudes - 20°C.

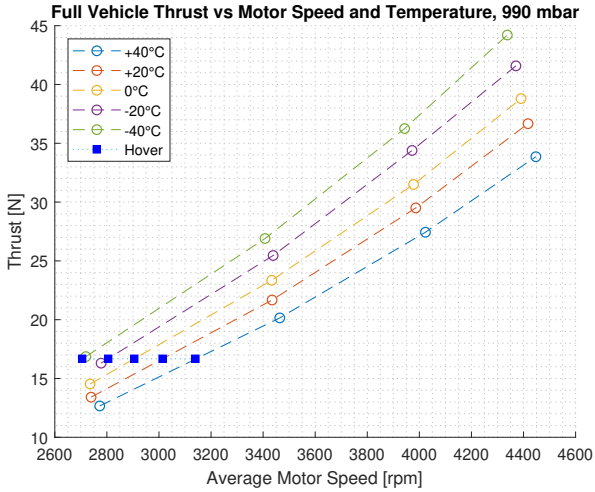

Fig. 14: Full vehicle thrust as a function of motor speed for all the temperatures - 990 mbar.

speed as well as power for the propeller and full vehicle. In total, 26 different climatic conditions are simulated (environmental matrix) to investigate the effect of temperature and pressure separately and their combinations.

Thrust and mechanical power are provided for the isolated rotor as a function of pressure (at constant temperature) and temperature (at constant pressure). Moreover, thrust and torque coefficients are reported for all the atmospheres set in the test section. The propeller thrust coefficient shows a linear dependence on Reynolds number, while the torque (and power) coefficient is almost constant. The c_T experiences a 16% increase as the Reynolds is increased (high temperature and low altitude) in accordance with the experimental studies available in literature.

The full vehicle thrust and electrical power curves are given to show the effect of pressure and temperature. As in the isolated rotor tests, the complete UAS Thrust vs Motor Speed curve shows a parabolic behaviour with decreasing concavity as high altitudes or temperatures are set. The air density changes affect both the thrust generated by the multicopter and the speed of each motor. High altitudes result in more electrical power required to hover the UAS; low temperatures show slower motor speed and reduced power required to achieve the hover thrust.

Moreover, the thrust coefficient is computed for the environmental matrix simulated in the test facility. The multirotor c_T shows a linear dependence on Reynolds number. The higher the Reynolds, the higher the thrust coefficient owing to improved aerodynamic field conditions and limited effect of viscous forces. The full vehicle c_T percent increase is close to the isolated rotor percent change; furthermore, the electrical power coefficient is almost constant, in accordance to the torque coefficient computed for the isolated rotor.

Future works include the characterization of a commercial

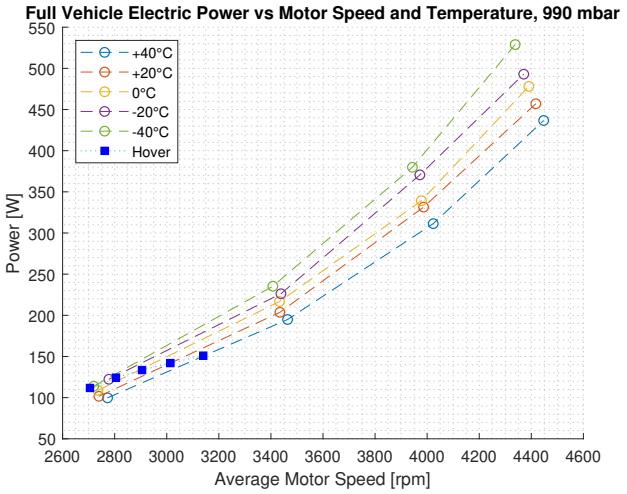

Fig. 15: Full vehicle electrical power as a function of motor speed for all the temperatures- 990 mbar.

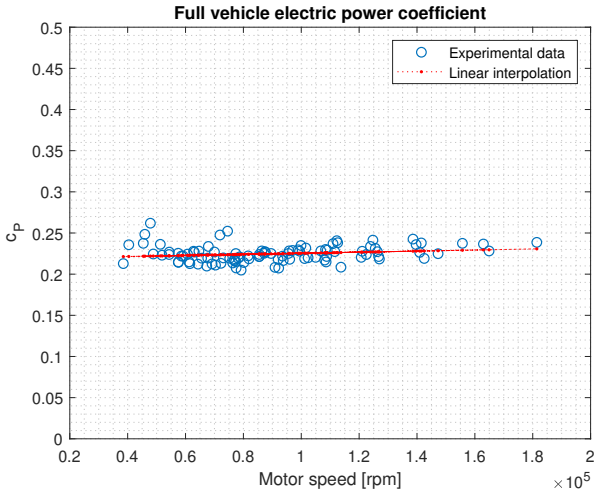

Fig. 17: Full vehicle electrical power coefficient as a function of Reynolds number for all the environmental conditions.

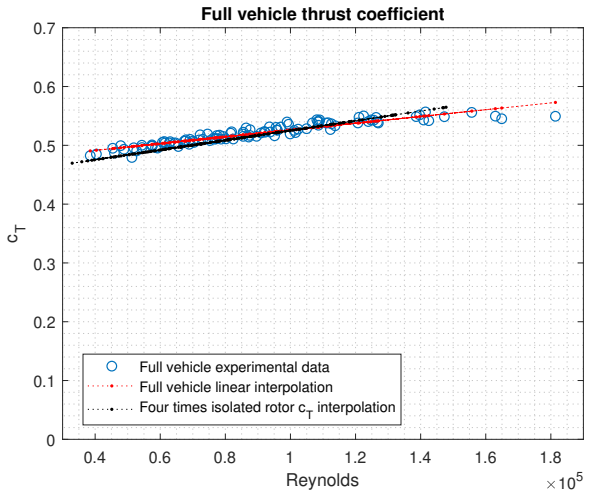

Fig. 16: Full vehicle thrust coefficient as a function of Reynolds number for all the environmental conditions.

UAS autopilot, including accelerometer as well as gyroscope noise with respect to temperature and barometer performance at high altitudes. Moreover, the efficiency of brushless motors with respect to air temperature will be investigated to make an estimate of the full vehicle mechanical power coefficient given the electrical power delivered by the power supply. Finally, additional test scenario, such as wind at low pressure and temperature, will be explored to overcome current experimental setup limitations and leverage the capabilities of terraXcube simulator.

ACKNOWLEDGMENT

The research leading to these results has received funding from the European Regional Development Fund 2014-2020 of , under Grant Agreement 2223/2017/Project number FESR1048, Creazione di un servizio di sviluppo tecnico per droni testati per il funzionamento in condizioni ambientali estreme, DronEx.

REFERENCES

[1] González-Jorge, H., Martínez-Sánchez, J., & Bueno, M. (2017). Unmanned aerial systems for civil applications: A review. Drones, 1(1), 2.

[2] Bloise, N., Primatesta, S., Antonini, R., Fici, G. P., Gaspardone, M., Guglieri, G., & Rizzo, A. (2019, June). A Survey of Unmanned Aircraft System Technologies to enable Safe Operations in Urban Areas. In 2019 International Conference on Unmanned Aircraft Systems (ICUAS) (pp. 433-442). IEEE.

[3] Capello, E., Park, H., Tavora, B., Guglieri, G., & Romano, M. (2015, November). Modeling and experimental parameter identification of a multicopter via a compound pendulum test rig. In 2015 Workshop on Research, Education and Development of Unmanned Aerial Systems (RED-UAS) (pp. 308-317). IEEE.

[4] Logan, M. J., & Glaab, L. J. (2017). Failure mode effects analysis and flight testing for small unmanned aerial systems. In 17th AIAA Aviation Technology, Integration, and Operations Conference (p. 3270).

[5] Deters, R. (2014). Performance and slipstream characteristics of small-scale propellers at low Reynolds numbers (Doctoral dissertation, University of Illinois at Urbana-Champaign).

[6] Lorefice, L., Pralio, B., & Quagliotti, F. (2004). Fluorescent oil flow visualization technique applied to 2D airfoils at very low Reynolds numbers. In 2004 International Symposium on Flow Visualization.

[7] W.J.M. Rankine. On the mechanical principles of the action of propellers. 6th session of the Institution of Naval Architects, (9):13–19, 1865.

[8] R. E. Froude. On the part played in propulsion by differences of fluid pressure. Trans. Inst. Nav. Arch., 30:390, 1889

[9] Brandt, John, and Michael Selig. Propeller performance data at low reynolds numbers. 49th AIAA Aerospace Sciences Meeting including the New Horizons Forum and Aerospace Exposition, 2011.

[10] Russell, Carl R., et al. Wind Tunnel and Hover Performance Test Results for Multicopter UAS Vehicles, 2016.

[11] Zawodny, N. S., & Boyd, D. D. (2020). Investigation of Rotor–airframe Interaction Noise Associated with Small-Scale Rotary-Wing Unmanned Aircraft Systems. Journal of the American Helicopter Society, 65(1), 1-17.

[12] Zhou, W., Ning, Z., Li, H., & Hu, H. (2017). An experimental investigation on rotor-to-rotor interactions of small UAV propellers. In 35th AIAA applied aerodynamics conference (p. 3744).

[13] Russell, C. R., & Sekula, M. K. (2017). Comprehensive Analysis Modeling of Small-Scale UAS Rotors.

[14] DronEx: Testing drones in extreme environmental conditions. Retrieved January, 2019, from https://terraxcube.eurac.edu/projects/dronex/

[15] Scanavino, M., Vilardi, A., & Guglieri, G. An Experimental Analysis on Propeller Performance in a Climate-controlled Facility. Journal of Intelligent & Robotic Systems, 1-13.s

[16] terraXcube Eurach Research. Retrieved January, 2020, from https://terraxcube.eurac.edu/
[17] RCBenchmark 1585. Retrieved January, 2020, from https://www.rcbenchmark.com/pages/series-1580-thrust-stand-dynamometer
[18] Q4L UAV. Retrieved January, 2020, from https://www.mavtech.eu/it/azienda/fuori-produzione/
[19] T-Motor 3508 KV 380. Retrived Jannuary, 2020, from http://store-en.tmotor.com/goods.php?id=354
[20] Thrust and Dynamometer - How to measure torque. Retrived Jannuary, 2020, from https://docs.rcbenchmark.com/en/faq.html
[21] Theys, B., Dimitriadis, G., Hendrick, P., & De Schutter, J. (2016, June). Influence of propeller configuration on propulsion system efficiency of multi-rotor Unmanned Aerial Vehicles. In 2016 international conference on unmanned aircraft systems (ICUAS) (pp. 195-201). IEEE.
[22] Conyers, Stephen A., Matthew J. Rutherford, and Kimon P. Valavanis. An Empirical Evaluation of Ground Effect for Small-Scale Rotorcraft. 2018 IEEE International Conference on Robotics and Automation (ICRA). IEEE, 2018.
[23] Conyers, Stephen A., Matthew J. Rutherford, and Kimon P. Valavanis. An empirical evaluation of ceiling effect for small-scale rotorcraft. 2018 International Conference on Unmanned Aircraft Systems (ICUAS). IEEE, 2018.
[24] Jain, S., Sitaram, N., & Krishnaswamy, S. (2015). Effect of Reynolds number on aerodynamics of airfoil with Gurney flap. International Journal of Rotating Machinery, 2015.
[25] JR3 Force/Torque Sensor. Retrived Jannuary, 2020, from https://www.jr3.com/resources/specification-sheets
[26] Sick photoelectric sensor WLA16P. Retrived Jannuary, 2020, from https://www.sick.com/it/it/sensori-fotoelettrici/sensori-fotoelettrici/w16/wla16p-24162100a00/p/p512654